Formation of Pyrophoric α-Fe Nanoparticles from Fe(II)-Oxalate

Rajesh Shende,[*] Alok Vats,[*] Zac Doorenbos,[*] Deepak Kapoor,[**] Christopher Haines,[**] Darold Martin,[**] and Jan Puszynski[*]

[*]Department of Chemical and Biological Engineering,
South Dakota School of Mines & Technology,
Rapid City, SD 57701 USA, Jan.Puszynski@sdsmt.edu
[**]Armament Research, Development, and Engineering Center
Picatinny Arsenal, NJ, 07806 USA

ABSTRACT

The formation of pyrophoric Fe-nanoparticles from Fe(II)-oxalate decomposition under H_2 atmosphere was investigated. The oxalate was synthesized by controlled nucleation process involving addition of oxalic acid in the $FeCl_2.2H_2O$ solution followed by separation and drying. As-synthesized oxalate was decomposed in a quartz tubular reactor at 450-520°C and reduced with a gases mixture containing 5 vol% of H_2 in N_2. After exposing it to air at room temperature, the fine Fe particles generated a temperature of about 800°C in less than 1 sec. In other approach, Fe-oxalate nanorods were synthesized by solid state synthesis method using polyethylene glycol surfactant. TEM images indicated nanorod like morphology with the diameter of about 20 nm and length of 70-80 nm. The fine oxalate particles were embedded in a porous Y_2O_3 matrix coated on a metallic substrate and reduced at the experimental condition stated above. Upon exposure to air, these substrates were found to be extremely reactive.

Keywords: Fe-oxalate, synthesis, nanorods, α-Fe, reactive substrate

1 INTRODUCTION

Iron (Fe), the most ubiquitous transition metal abundantly available in the Earth's crust, is the structural backbone of our modern infrastructure. It is therefore paradoxical that as a nanoparticle, Fe has been somewhat neglected in favor of other metals such as Au, Ag, Pt, Ni, Cu etc. This is understandable because Fe is extremely reactive. Fe as fine particles have long been known to be pyrophoric [1], which might be the major reason that Fe nanoparticles have not been fully investigated. Fe nanoparticles have several important applications in catalysis [2], magnetic resonance imaging [3], magnetic data storage [4], coatings [5], synthesis of carbon nanotubes [6], synthesis of highly oriented and ordered nanostructures for field emission devices [7] etc. Further research is currently being pursued to explore electrical, dielectric, magnetic, optical, imaging, catalytic, biomedical and bioscience properties of Fe nanoparticles.

Although fine Fe particles have been long known as pyrophoric, only few studies [8-10] investigated the pyrophoric behavior of Fe nanoparticles. These reactive nanoparticles can be produced by thermal decomposition of Fe precursor [11], selective leaching of a metal from an alloy [9], e.g. Fe-Al, and reduction of Fe compounds such as oxides or oxalates in H_2 environment. Recently, Lawrence Livermore National Laboratory (LLNL) has developed the sol-gel methodology to generate high surface area porous Fe [8]. These investigators however, found out that the porous Fe prepared by sol-gel route is non-pyrophoric but ignitable by thermal source. They believe that the addition of W or Sn particles to the sol-gel derived Fe nanoparticles can improve their pyrophoric action [8]. Other investigators [9] have studied the reduction of Fe-oxalate in H_2 atmosphere to produce α-Fe nanoparticles. These nanoparticles were non-pyrophoric but they were very effective for scavenging O_2 from Ar atmosphere [12]. α-Fe, however, has been reported to be the most active form of Fe that is pyrophoric [8-10].

Very recently, we reported the synthesis of pyrophoric particles from micron size Fe-oxalate particles [10]. These particles were produced by thermal decomposition followed by reduction of Fe-oxalate in the H_2 environment. In the present investigation, we report synthesis of Fe-oxalate nanoparticles using $FeCl_2.2H_2O$ and oxalic acid in presence of polyethylene glycol surfactant. In using a surfactant the nucleation will occur inside the micelles, which will produce well-defined nanostructures such as nanorods. Although the synthesis of oxalate nanorods using the reverse micellar route employing cetyltrimethyl ammonium bromide surfactant has been reported [11], the synthesis of pyrophoric nanoparticles from the oxalate nanorods has not been reported so far. This study further includes the embodiment of oxalate particles inside Y-OOH gel to fabricate the reactive substrates. The results presented here exhibit the pyrophoric response of the active Fe produced by thermal decomposed followed by reduction in H_2 and N_2 environment.

2 EXPERIMENTAL

2.1 Materials

Ferrous chloride ($FeCl_2.2H_2O$) and oxalic acid (HOOCCOOH) used for the synthesis of Fe-oxalate were procured from Sigma-Aldrich, WI. The PEG-600 surfactant used to prepare nanoscale oxalate powder was obtained from Alfa-Aeser. Yttrium chloride ($YCl_3.7H_2O$), ethanol, Brij-76 surfactant and propylene oxide required to prepare mesoporous gel were procured from Sigma Aldrich (WI). Stainless steel foils were purchased from McMaster Carr.

2.2 Synthesis of Fe(II)-oxalate

In one synthesis approach, $FeCl_2.2H_2O$ was dissolved in de-ionized water and the solution was heated to 60-70°C under magnetic stirring. Oxalic acid was dissolved in de-ionized water and the solution was added drop wise to the $FeCl_2.2H_2O$ solution. After addition, the contents were maintained for 2 h under constant stirring. The solution mixture was allowed to cool down to the room temperature and the contents were centrifuged to recover the precipitate. Synthesis of Fe-oxalate nanorods was attempted using polyethylene glycol (PEG-600) surfactant. In this, oxalic acid, $FeCl_2.2H_2O$ and PEG-600 were homogeneously mixed together for about 30 min. The contents were diluted with de-ionized water and ethanol, sonicated for 4 h and finally centrifuged to recover the precipitate.

2.3 Synthesis of Y-OOH gel embedded with Fe-oxalate particles

To synthesize the Y-OOH gel, Solution-A containing $YCl_3.7H_2O$ in ethanol and Solution-B of Brij-76 (20-30 wt%) in ethanol were prepared by ultrasonic mixing. Solution-B was added drop wise to the Solution-A and after mixing these two solutions at room temperature, propylene oxide was added, which resulted in a transparent gel in 5 min. The gel was aged for 1-2 hrs and Fe-oxalate powder was added to it. This synthesis route is designated as route-I. The oxalate loading was varied between 30-80 wt% based on the weight of YCl_3 initially taken. In another synthesis route, designated as route-II, the oxalate powder was first dispersed in the solution mixture of Solution-A and Solution-B and later, propylene oxide was added to achieve the gel formation. The time required for the gel formation was 5-6 min.

2.4 Fabrication of reactive substrate

Fabrication involves dip coating a metallic foil with a Y(yttrium)-sol solution followed by coating a layer of the oxalate and finally, dip-coating this foil in Y-sol solution. To synthesize the Y-sol solution, $YCl_3.7H_2O$ and Brij-76 (20-30 wt%) were dissolved in ethanol by ultrasonic mixing and propylene oxide was added. A metallic foil was dip coated with this Y-sol solution. The films were annealed at 100°C for 5 min. Next, Fe(II)-oxalate slurry in acetone containing 20wt% polycarbonate binder was prepared and applied on the dip-coated Y-OOH sol solution using a doctor blade casting technique. After drying the film for few minutes, the metallic foil previously coated with the oxalate was dip coated in Y-sol solution and dried at 90°C.

2.5 Thermal decomposition, reduction, and oxidation

The decomposition experiments were performed in an isothermal flow reactor where Fe(II)-oxalate powder or foil was placed inside a quartz tube supported in a split furnace. The quartz tube was connected with two mass flow controllers to monitor the flow rates of H_2 and N_2 gases. Oxalate sample was heated to 450-500°C under the constant flow of N_2 and reduced with H_2 (5 vol%) for 5 min. The sample was cool down to the room temperature under the flow of N_2. The α-Fe samples removed from the reactor and exposed to air at ambient conditions to allow it to undergo oxidation. The temperature was continuously recorded using a pyrometer mounted on the tubular flow reactor.

2.6 Characterization

As-synthesized oxalate powder, nanorods, and commercial oxalates were analyzed by Fourier transform infrared (FTIR) spectroscopy. Microstructural characterization of various samples was performed using scanning and transmission electron microscopy.

3 RESULTS AND DISCUSSION

The FTIR spectra of as-synthesized Fe-oxalate showed the –CO and –OCO vibrations of the oxalate ligand at 1636 and 800 cm^{-1}, respectively whereas the bridging vibrations of oxalate were found in the region of 1370-1300 cm^{-1}. Absorption corresponding to Fe was observed in the region of 480-520 cm^{-1}. The other characteristics signatures of the as-synthesized oxalate were similar to the commercial oxalate samples.

The as-synthesized oxalate was thermally decomposed, reduced in a tubular quartz reactor, and finally, exposed to ambient air allowing α-Fe to undergo oxidation as per the procedure outlined in the Experimental section. The effect of reducing environment on the peak temperature (T_{peak}) generated during oxidation of α-Fe is shown in Figure 1. It can be observed that when 100vol% H_2 was used at the decomposition temperature of 500°C, the peak temperature produced during oxidation was around 600°C. However, while decomposing the oxalate at the same temperature but reducing with 5vol% H_2, the T_{peak} was increased to 735°C.

At 450°C decomposition temperature and using 5vol% H$_2$, the T$_{peak}$ decreased to about 400°C. Thus, we selected H$_2$ of 5 vol% with 95 vol% N$_2$ as the most effective reducing environment.
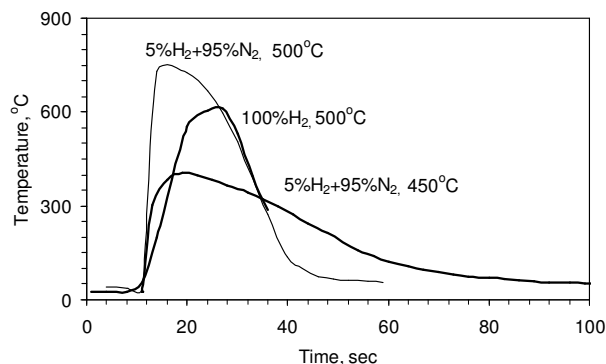

Figure 1: Transient temperature profile of the obtained from oxidizing the a-Fe produced from reducing the Oxalate at various processing conditions.

Mechanism of Fe-oxalate decomposition and reduction is rather complex involving several reactions. Thermal decomposition of oxalate dihydrate leads to dehydration at low temperatures up to about 200°C [10]. In presence of H$_2$, oxalate reduces to FeO (unstable), which further reduces to Fe$_3$O$_4$ and finally it leads to α-Fe. The gaseous products produced concomitantly with FeO further reacts with Fe to form Fe$_3$C that reduces to Fe and CH$_4$. We have also performed thermal decomposition, reduction, and oxidation of α-Fe obtained from Fe$_2$O$_3$ and Fe$_3$O$_4$, and the T_{peak} observed are given in Table 1, which also summarizes T_{peak} for the commercial oxalates. We can notice that the T$_{peak}$ generated by oxidation of the α-Fe produced from as-synthesized oxalate is around 800°C, which is the maximum among those reported in the table.

Compound	Source	H$_2$, vol%	T$_{peak}$, ^{o}C
Fe$_2$O$_3$	Alfa-Aesar	5	700 ± 25
Fe$_3$O$_4$	Alfa-Aesar	5	650 ± 20
F$_e$C$_2$O$_4$.2H$_2$O	Baker, NJ	5	620 ± 10
F$_e$C$_2$O$_4$.2H$_2$O	Sigma Aldrich	10	560 ± 05
F$_e$C$_2$O$_4$.2H$_2$O	As-synthesized	5	800 ± 10

Table 1 Peak temperature (T_{peak}) observed during oxidation of pyrophoric α-Fe

Scanning electron microscopy (SEM) images of as-synthesized Fe-oxalate and after reduction and oxidation are shown in Figure 2a and b. The microstructure reveals plate and rod-like particle morphology. These plates and rods are few μm in size and they are stacked together. TEM image of as-synthesized nanoscale oxalate is shown in Figure 3, which shows nanorod morphology. Under higher

resolution the majority of nanorods were found to have an aspect ratio of approx. 3.0. Oxidation of α-Fe produced from the decomposition of oxalate nanorods was found to be pyrophoric as well.
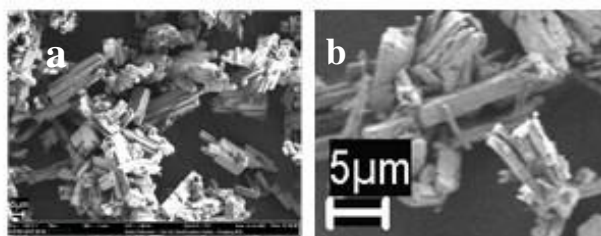

Figure 2: SEM images of the oxalate a) as-synthesized, and b) after reduction and oxidation.
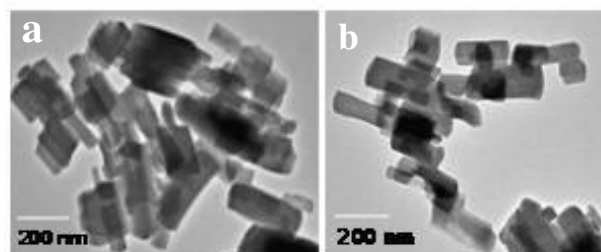

Figure 3: SEM images of the oxalate nanorods a) as-synthesized, and b) after dispersion in ethanol.

Y-OOH gels containing the oxalate were prepared by using the two synthesis routes as elaborated in the Experimental section. In route-I, the oxalate was added to the Y-OOH gel whereas, in route-II, the oxalate was initially dispersed in the Y-sol-solution and later the gelation was achieved using propylene oxide. Fe-oxalate was added to the gel in the amount of 30-80% (w/w) based on the YCl$_3$ weight originally taken. The gels prepared by synthesis route-I were decomposed to 500°C in N$_2$ atmosphere and reduced in presence of 5 Vol% H$_2$. The transient temperature profiles obtained after exposing the gel containing the reduced oxalate to ambient air are shown in Figure 4.
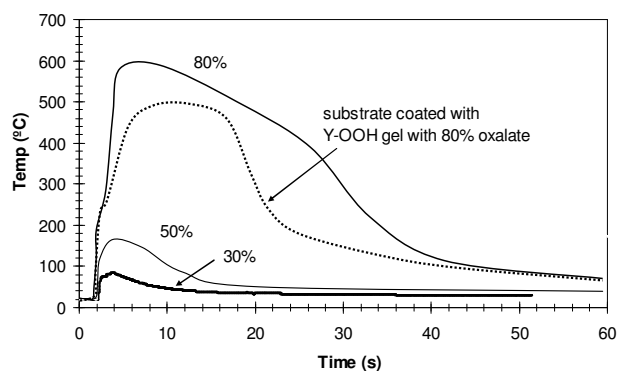

Figure 4: Transient temperature profiles obtained from air oxidation of α-Fe produced from reducing the Y-OOH gels mixed with the oxalate in the amount of 30-80% (w/w).

We can observe that the T_{peak} for the gels mixed with the oxalate increases as the loading of the oxalate increases from 30 to 80% (w/w). At the level of 30 wt% oxalate mixed with Y-OOH gel, the temperature barely reach to $100^{o}C$ whereas for 80 wt% oxalate, the temperature increased to $600^{o}C$. Another important observation is that the temperature sustained for longer time at the higher levels of the oxalate, which is obvious because the active Fe content produced from higher loadings of the oxalate is higher.

In other experiments, the gels prepared with the synthesis route-II (where propylene oxide addition was performed after dispersing the oxalate in Y-sol solution) were heated to $500^{o}C$ in N_2 atmosphere and reduced in presence of 5 Vol% H_2. After exposing α-Fe to air, the T_{peak} obtained by this route were lower than route-I where oxalate was added to Y-OOH gel previously made with propylene oxide. It is possible that the propylene oxide may have degrading effect on the oxalate converting it at least partly into its oxide and α-Fe produced from the oxide is less pyrophoric than the one generated from the oxalate (Table 1).

The pyrophoric response of Y-OOH film loaded with 80%oxalate and coated on a metallic substrate is shown in also shown in Figure 4. The T_{peak} generated during oxidation of reduced film is around $550^{o}C$, which is slightly lower than the T_{peak} achieved for the Y-OOH gel mixed with the oxalate at 80% concentration level (Figure 1). In the green state, the film was free of any cracks; however, during decomposition and reduction, several cracks were developed. The thickness of the films prepared by doctor blade type of casting technique was approx. 300 μm. We believe that the longer path length for the diffusion of gas species produced during decomposition might be the cause for the crack formation. Currently, we are making efforts to develop defect free reactive substrates containing Fe-nanoparticles.

4 CONCLUSIONS

Synthesis of Fe-oxalate in the form of nanorods has been accomplished using a controlled nucleation process using $FeCl_2$ and oxalic acid with the use of PEG-600 surfactant. The aspect ratio of the as-synthesized nanorods was about 3.0. The α-Fe produced after decomposition and reduction of the micron and nano size oxalates at $500^{o}C$ using 5vol%H_2 was found to be reactive in air as the pyrophoric temperature as high as $800^{o}C$ was achieved. The films fabricated by coating the Y-OOH gel embedded with Fe-oxalate on a metallic substrate were found to be reactive as well.

ACKNOWLEDGEMENT

REFERENCES

[1] E.A. Shafranovsky,Yu. I. Petrov . "Aerosol Fe Nanoparticles with the Passivating Oxide Shell", Journal of Nanoparticle Research. 6, 1, 71-90, 2004.

[2] Xuanke Li, Zhongxing Lei, Rongcui Ren, Jing Liu, Xiaohua Zuo, Zhijun Dong, Houzhi Wang, Jianbo Wang, "Characterization of carbon nanohorn encapsulated Fe particles", Carbon, 41, 15, 3068-3072, 2003.

[3] Stefan G. Ruehm, Claire Corot; Peter Vogt, Stefan Kolb, Jörg F. Debatin, "Magnetic Resonance Imaging of Atherosclerotic Plaque With Ultrasmall Superparamagnetic Particles of Iron Oxide in Hyperlipidemic Rabbits" Circulation, 103 , 415-422, 2001.

[4] S. A. Majetich, Y. Jin, "Magnetization Directions of Individual Nanoparticles" Science, 284, 5413, 470 – 473, 1999.

[5] Satoshi Tomita, Masahiro Hikita, Minoru Fujii, Shinji Hayashi, Keiichi Yamamoto, "A new and simple method for thin graphitic coating of magnetic-metal nanoparticles", Chemical Physics Letters, 316(5-6),361-364, 2000

[6] Yoshikazu Homma, Takayuki Yamashita, Paul Finnie, Masato Tomita, Toshio Ogino, "Single-Walled Carbon Nanotube Growth on Silicon Substrates Using Nanoparticle Catalysts", Jpn. J. Appl. Phys., 41, L89-L91, 2002

[7] C. H. Liang, G. W. Meng, L. D. Zhang, Y. C. Wu, Z. Cui, "Large-scale synthesis of β-SiC nanowires by using mesoporous silica embedded with Fe nanoparticles", Chemical Physics Letters, 329, 3-4, 323-328, 2000.

[8] A.E. Gash, J.H. Satcher Jr., R. L. Simpson, "Preparation of porous pyrophoric iron using sol-gel method", US Patent 20060042417, Appl. No. 11/165734.

[9] US Patent 4435381, "Pyrophoric foil and article, and pyrophoric technique", Alloy Surfaces Company Inc., March 6, 1984.

[10] R. V. Shende, A. Vats, Z.D. Doorenbos, D. Kapoor, D. Martin, J.A. Puszynski, "Formation of pyrophoric iron particles by H_2 reduction of oxalates and oxides", 7th International Symposium on Special Topics in Chemical Propulsion, Kyoto, Japan, 2007.

[11] A.K. Ganguli, T. Ahmed, "Nanorods of iron oxalate synthesized using reverse micelles: facile route for alpha Fe_2O_3 and Fe_3O_4 nanoparticles", J. Nanoscience Nanotechnology, 7, 6, 2029, 2007.

[12] P. Pranda, V. Hlavacek, M.L. Markowski (2002) "Ultrafine iron powder as an oxygen scavenger for argon purification", Ind. Eng. Chem. Res., 41, 4837, 2002.